

Statistics of Dissipation and Enstrophy Induced by a Set of Burgers Vortices

Guowei He^{1,4}, Shiyi Chen^{1,2}, Robert. H. Kraichnan³, Raoyang Zhang¹, and Ye Zhou²

¹*Theoretical Division and Center for Nonlinear Studies, Los Alamos National Laboratory, Los Alamos, NM 87545*

²*IBM Research Division, T. J. Watson Research Center, P.O. Box 218, Yorktown Heights, NY 10598*

³*396 Montezuma 108, Santa Fe, New Mexico, 87501-2626,*

⁴*LNM, Institute of Mechanics, Chinese Academy of Sciences, Beijing, 100080, P. R. China*

Dissipation and enstrophy statistics are calculated for an ensemble of modified Burgers vortices in equilibrium under uniform straining. Different best-fit, finite-range scaling exponents are found for locally-averaged dissipation and enstrophy, in agreement with existing numerical simulations and experiments. However, the ratios of dissipation and enstrophy moments supported by axisymmetric vortices of any profile are finite. Therefore the asymptotic scaling exponents for dissipation and enstrophy induced by such vortices are equal in the limit of infinite Reynolds number.

Recent direct numerical simulations (DNS) [1] have revealed spatial structures with regions of intense dissipation density $\epsilon = \frac{1}{2}\nu(\partial u_i/\partial x_j + \partial u_j/\partial x_i)^2$ and enstrophy density $\Omega = \omega^2$, where ν is kinematic viscosity, $\omega = \nabla \times \mathbf{u}$ is vorticity, and \mathbf{u} is the fluid velocity. The spatial distributions of enstrophy density and dissipation density are qualitatively different. Intense vorticity has a tube-like (or filament-like) structure, while intense dissipation typically surrounds the vortex tubes and forms double-peak structures centered on the tubes. This difference of structure implies differences in intermittency between enstrophy and dissipation and has been linked to a difference between the empirical scaling exponents of longitudinal and transverse structure functions recently observed in experimental measurements [2–5] and DNS [6–8].

Siggia [9], Kerr [10], and Meneveau et al. [11] have noted that enstrophy is more intermittent than dissipation. More recently, Chen et al. [6] used DNS data to calculate empirical scalings of enstrophy and dissipation. They found that the exponents for locally-averaged enstrophy were significantly smaller than those for locally-averaged dissipation and related the differences to an elaboration of Kolmogorov's refined similarity hypothesis.

Traditional experimental measurements typically invoke Taylor's hypothesis and the calculation of inertial-range scaling exponents can be contaminated by large-scale shear effects. DNS using the largest available computers can reach only moderate Reynolds, at which the inertial range is narrow. These difficulties accentuate the need for theoretical understanding of intermittency phenomena and their role in scaling.

Distributions of idealized vortices have been used by a number of authors to model turbulence statistics. The hope here is that the vortex distribution can characterize both the essential physics of the small-scale structures and the observed vorticity statistics, thereby leading to an acceptable description of overall turbulence properties. Idealized vortices that have been studied include the Hill vortex [12], simple vortex filaments [13], the Burgers vortex [14], and spiral vortices [14]. A distribution

of modified Burgers vortices will be used in the present paper to model scaling exponents over finite ranges. Before presenting detailed results for the Burgers vortex, we shall discuss the underlying question of whether cylindrical vortex structures can support different asymptotic scaling exponents for enstrophy and dissipation.

Moments of locally averaged enstrophy and dissipation densities in a velocity field with isotropic overall statistics may be defined by

$$\Omega_n(\ell) = \langle [\Omega]_\ell^n \rangle, \quad \epsilon_n(\ell) = \langle [\epsilon]_\ell^n \rangle, \quad (1)$$

where $\langle \rangle$ denotes ensemble average over the isotropic statistics and $[]_\ell$ denotes space average over a region of characteristic linear dimension ℓ . Joint powerlaw scaling with enstrophy exponents ζ_n and dissipation exponents ξ_n exists if there is a range of ℓ in which

$$\Omega_n(\ell) \propto (L/\ell)^{\zeta_n}, \quad \epsilon_n(\ell) \propto (L/\ell)^{\xi_n}, \quad (2)$$

Here L is a macroscale that marks the bottom of the scaling range. The space averaging $[]_\ell$ smears spots of intense excitation. Therefore ζ_n and ξ_n are expected to be positive. Let ℓ_d mark the top of the scaling range, which we assume is also the beginning of the dissipation range.

Suppose that $0 < \xi_n < \zeta_n$ and that the length of the scaling range in decades becomes infinite in the limit $Re \rightarrow \infty$ where Re is a turbulence Reynolds number. Then $\Omega_n(\ell_d)/\epsilon_n(\ell_d) \rightarrow \infty$ as $Re \rightarrow \infty$. A corollary is that the ratio of single-point averages becomes infinite in the limit: $\langle \Omega^n \rangle / \langle \epsilon^n \rangle \rightarrow \infty$. We assume here that $\langle \epsilon^n \rangle / \epsilon_n(\ell_d)$ does not become infinitely larger than $\langle \Omega^n \rangle / \Omega_n(\ell_d)$. Now we can ask what kind of vortex structure, if any, can support this behavior. If $\langle \Omega^n \rangle / \langle \epsilon^n \rangle$ goes infinite, where the averages are over the entire field, then there must be at least one vortex structure in the field for which the ratio of averages over that single structure goes infinite.

A cylindrical vortex is characterized by the azimuthal velocity $v_\theta(r)$, where r is distance from the vortex axis.

The enstrophy density and dissipation density (normalized by ν) are

$$\Omega(r) = \left(\frac{dv_\theta}{dr} + \frac{v_\theta}{r} \right)^2, \quad \epsilon(r) = \left(\frac{dv_\theta}{dr} - \frac{v_\theta}{r} \right)^2. \quad (3)$$

The enstrophy and dissipation per unit length of vortex are $2\pi \int_0^\infty \Omega(r)r dr$ and $2\pi \int_0^\infty \epsilon(r)r dr$, respectively. The moments

$$\Omega_n = 2\pi \int_0^\infty [\Omega(r)]^n r dr, \quad \epsilon_n = 2\pi \int_0^\infty [\epsilon(r)]^n r dr \quad (4)$$

describe the distribution of enstrophy and dissipation densities in the single vortex structure. By (3), $\Omega_1 = \epsilon_1$ if $v_\theta(0) = v_\theta(\infty) = 0$

Consider first the Rankin vortex of radius r_0 for which $v_\theta \propto r$ ($r < r_0$) and $v_\theta \propto 1/r$ ($r > r_0$). Here the vorticity is confined to a rigidly rotating core and all the dissipation lies outside the core. The ratios $R_n = \Omega_n/\epsilon_n$ calculated from (3) are $R_n = 2n - 1$.

For the Burgers vortex of radius r_b ,

$$v_\theta(r) = \frac{\Gamma}{2\pi} \frac{1 - \exp(-r^2/r_b^2)}{r}, \quad (5)$$

where Γ is the total circulation. By (3), $\Omega(r) \propto \exp(-2r^2/r_b^2)$, and the vorticity and dissipation now overlap. Eq. (3) yields $R_2 \approx 10.65$, $R_3 \approx 104.07$, $R_4 \approx 1040.02$. To a rough approximation, $R_n \sim 10^{n-1}$.

The cylindrical vorticity distribution that maximizes R_2 can be found by solving the associated variational problem, with $\int_0^\infty \omega(r)r dr$ and Ω_1 held constant. The result confirms what can be guessed by inspection of (3): The maximizing distribution is the limit $r_0 \rightarrow \infty$ of

$$v_\theta(r) \propto r \quad (r < r_0), \quad v_\theta(r) \propto r^\alpha \quad (r_0 < r < r_1), \\ v_\theta(r) \propto 1/r \quad (r > r_1), \quad (6)$$

with $\alpha = 1/2$. In this case, $R_n = (n-1)9^n$ for $n > 1$. The essential facts here are first, if $v_\theta \propto r^\alpha$, then $\Omega(r)/\epsilon(r)$ grows as $\alpha \rightarrow 1$; second, $\alpha = 1/2$ is the largest α for which $\int_{r_0}^{r_1} [\Omega(r)]^2 r dr$ diverges as $r_0 \rightarrow 0$, thereby making the relative contribution to ϵ_2 from the $v_\theta \propto 1/r$ region negligible in the limit. The maximum R_n for $n > 2$ also are finite; they are maximized at α values that increase with n .

It follows that differing asymptotic scaling exponents for enstrophy and dissipation cannot be supported by cylindrical vortices. The vortex profile that maximizes R_2 is one in which $\omega(r)$ is highly diffuse and the dominant contributions to $[\Omega(r)]^2$ and $[\epsilon(r)]^2$ have the same r dependence. This refutes the intuition that the maximizing distribution is one in which a compact vortex core is surrounded by diffuse dissipation.

Similar arguments establish that differing asymptotic scaling exponents for longitudinal and transverse structure functions [15] cannot be supported by cylindrical vortices.

If the cylindrical vortex is replaced by a plane vortex layer, it is trivial that all $R_n = 1$. This suggests that the cylindrical vortex may be the form that maximizes the R_n . In any event, we conjecture that the R_n are finite whatever the shape of the finite volume that is filled with the intense vorticity.

The Navier-Stokes (NS) equation so far has not been invoked. Highly diffuse cylindrical vortices are not expected to survive under the NS equation; the value $R_2 = 10.65$ for the Burgers vortex plausibly is closer to the maximum R_2 attainable under NS.

In the remainder of this paper, a distribution of modified Burgers vortices will be constructed in order to demonstrate that different finite-range scaling exponents for enstrophy and dissipation can be realized despite the fact that the infinite-range exponents must be equal. Data from experiments and DNS are invoked in the construction, but the model is essentially artificial and we do not offer it as a realistic representation of the vortex structure of actual turbulence.

Exponential-like distributions of vortex core radii have been observed in DNS by Jimenéz et al. [19] and in an experiment by Tabeling et al. [21]. We introduce a distribution of core sizes into our model by fitting the high-Reynolds number data in [21] to a stretched exponential, thereby obtaining the radius pdf

$$P(r_b) \propto \eta^{-3} r_b^2 \exp[-(r_b/\eta)^{0.7}], \quad (7)$$

where η is an assumed Kolmogorov dissipation length [22]. Of course the experimentally observed vortex cores are not Burgers vortices.

The Burgers vortex (5) is in equilibrium under the NS equation if it lies within a uniform background strain field with radial and axial strain components $-a$ and a , such that $r_b = (2\nu/a)^{1/2}$. Here ν is kinematic viscosity. This background field has no vorticity but it does contribute to the total dissipation density, which becomes

$$\epsilon(r) = 12a^2 + \left(\frac{dv_\theta}{dr} - \frac{v_\theta}{r} \right)^2. \quad (8)$$

We consider a distribution of isolated Burgers vortices, each in its own background field. The ensemble average $\langle \rangle$ is over the radius pdf (7). The local averaging $[]_\ell$ invoked in (1) is realized as the average over a cylinder of radius ℓ and length 2ℓ , centered on a point \mathbf{x} in the space surrounding a vortex and aligned with the axis of the vortex, followed by an average over \mathbf{x} . In order to have finite total dissipation per unit core length according to (8), the integration over \mathbf{x} is extended only to a finite distance r_{max} from the vortex axis. This truncation is in lieu of taking account of vortex interactions and making

realistic changes in the straining field far from the vortex core.

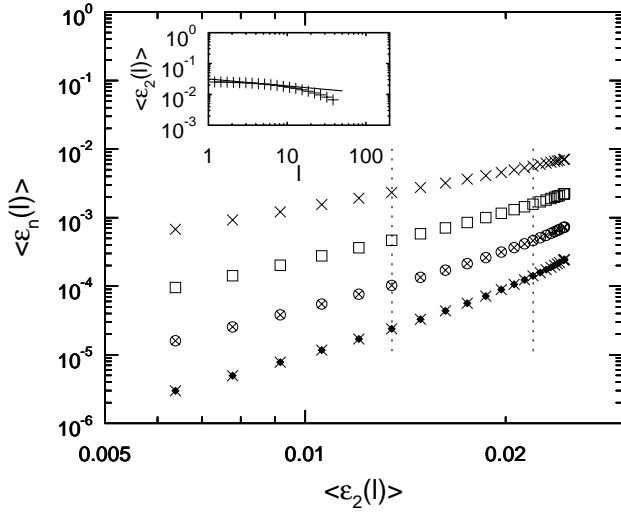


FIG. 1. Parametric plot of $\epsilon_n(\ell)$ as a function of $\epsilon_2(\ell)$ for $n = 3, 4, 5$ and 6 (from top to bottom). Finite-range exponents used in Figs. 2 and 5 are best fits over the region between the two dashed lines. The inset shows $\epsilon_2(\ell)$ versus ℓ .

In the numerical study reported here, the space integrations needed to evaluate the $\Omega_n(\ell)$ and $\epsilon_n(\ell)$ were performed by a second-order trapezoidal scheme whose accuracy was verified. We have taken $r_{max} = 10\eta$ and have fixed the vortex Reynolds number at $R_\Gamma \equiv \Gamma/\nu = 1293$. These values, together with (7), (non-uniquely) make the inhomogeneous model satisfy the homogeneity relations $\Omega_1(\ell) = \epsilon_1(\ell)$. By (5), a change in the value of R_Γ does not affect the enstrophy scaling, but by (8) it does affect the relative scalings of enstrophy and dissipation.

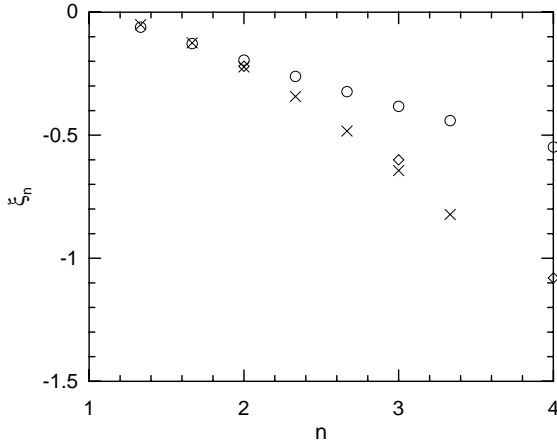


FIG. 2. The scaling exponents ξ_n of the locally averaged dissipation as a function of n : The circles represent our Burgers vortex model, the diamonds are data from an experiment by Sreenivasan et al. [23] and the crosses are DNS data [6].

Fig. 1 shows the $\epsilon_n(\ell)$ plotted against $\epsilon_2(\ell)$ for $n = 3, 4, 5$. A narrow powerlaw range can be identified. In

the inset, we plot $\epsilon_2(\ell)$ against ℓ . Local scaling exponents for dissipation and enstrophy are calculated as $\xi_n = d \ln \epsilon_n(\ell) / d \ln \ell$ and $\zeta_n = d \ln \Omega_n(\ell) / d \ln \ell$. The data used for Fig. 2 yield $\xi_2 = 0.195 \pm 0.0747$, which is not far from the value $2/9$ given by some simple scaling models or the experimental value 0.25 ± 0.05 [23].

Fig. 2 shows ξ_n versus n . For $n \leq 2$, the present model agrees well with the DNS and experimental data. For $n > 2$, the exponents from the present model decrease too slowly, indicating an unrealistic rate of increase of intermittency with decrease of scale.

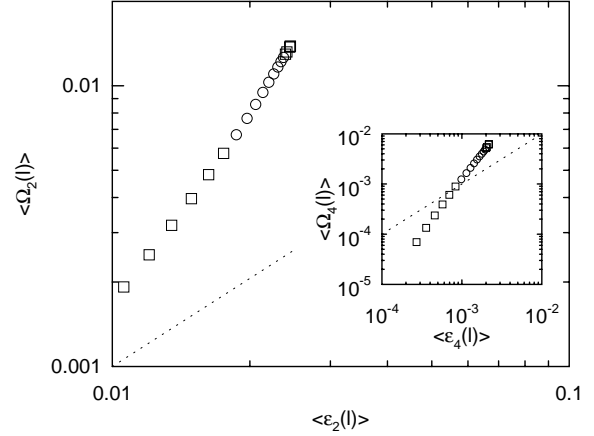


FIG. 3. Parametric plot of $\Omega_2(\ell)$ as a function of $\epsilon_2(\ell)$. The circles denote the part of the plot for which ℓ lies between the dashed lines of Fig. 1. The dotted line corresponds to $\Omega_2(\ell) = \epsilon_2(\ell)$. The inset is a similar plot of $\Omega_4(\ell)$ and $\epsilon_4(\ell)$.

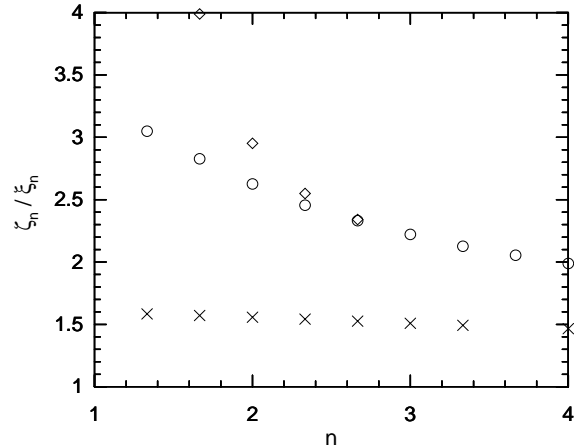


FIG. 4. Ratio of enstrophy and dissipation scaling exponents ζ_n / ξ_n as a function of n . The circles represent the present Burgers' vortex model, the diamonds are data from an experiment by Antonia et al [5], and the crosses are DNS data [6].

In Fig. 3, $\Omega_2(\ell)$ and $\Omega_4(\ell)$ are plotted against $\epsilon_2(\ell)$ and $\epsilon_4(\ell)$, respectively. Fig. 4 shows the ratio ζ_n / ξ_n as a

function of n for $4/3 \leq n \leq 4$. Data are presented for experiment [5], DNS [6], and the present model. The DNS was computed at mesh resolution 512^3 . The DNS ratio values in Fig. 4 decrease very slowly with increase of n . For the experimental data, the ratio values were calculated from measurements of longitudinal and transverse velocity structure functions by invoking refined similarity hypotheses for longitudinal velocity increments [24] and transverse velocity increments [6]. Experiment, DNS, and model all yield $\zeta_n/\xi_n > 1$.

We reach two principal conclusions. First, if the support of intense vorticity lies in cylindrical vortices, then differing asymptotic scaling exponents for locally-averaged enstrophy and dissipation are impossible. We do not see how this conclusion can be changed if the support lies in vortex structures of non-cylindrical shape. Second, models built on cylindrical vortices can yield differing finite-range scaling exponents [25]. It is plausible that compact cylindrical vortices do mediate the entropy intermittency measured at small scales. Moffatt et al [18] found, from an analysis of cylindrical vortices at a uniformly distributed angle to a constant strain field, that the vortex cores contained 63.3% of the total enstrophy and only 1.3% of the total enstrophy.

The Burgers vortex model presented here is arbitrary in a number of respects. Nevertheless, it is plausible that the filamentary vortex cores of actual turbulence are associated with moment ratios R_n that have orders of magnitude similar to those of the Burgers vortex. In this event, different best-fit scaling exponents for enstrophy and dissipation can be induced over substantial finite ranges of scales.

We thank H. Chen, M. Nelkin, K. R. Sreenivasan, Stefan Thomas, E. Titi and J. Z. Wu for useful discussions.

* Electronic address: ghe@t13.lanl.gov

[1] R. Brachet, Fluid Dyn. Research **8**, 1 (1991); G. R. Ruetsch and M. R. Maxey, Phys. Fluids A **4**, 2747 (1992); S. Kida and K. Ohkitani, Phys. Fluids A **4**, 1018 (1992), T. Passot, H. Politano, P. L. Sulem, J. R. Angilella and M. Meneguzzi, J. Fluid Mech. **282**, 313 (1995)).

[2] B. Dhruva, Y. Tsuji, and K. R. Sreenivasan, Phys. Rev. E, **56**, R4928 (1997).

[3] J. A. Herweijer and W. Van de Water, *Advances in turbulence*, V, edited by R. Benzi (Kluwer, Dordrecht) 210-216 (1995).

[4] R. 4, D. Barbagallo, D. Guj, and F. Stella, Phys. Fluids, **8**, 1181 (1996), R. Camussi, and R. Benzi, Phys. Fluids, **9**, 257, (1997).

[5] R. A. Antonia and B. R. Pearson, Europhys. Lett., **40**, 123 (1997).

[6] S. Chen, K. R. Sreenivasan, M. Nelkin and N. Cao, Phys. Rev. Lett., **79**, 1253 (1997), S. Chen, K. R. Sreenivasan and M. Nelkin, Phys. Rev. Lett. **79**, 2253 (1997).

[7] O. N. Boratav, Phys. Fluids **9**, 3120 (1997).

[8] S. Grossmann, D. Lohse and A. Reeh, submitted to Phys. Fluids (1997).

[9] E. Siggia, J. Fluid Mech., **107**, 375 (1981).

[10] R. Kerr, J. Fluid Mech., **153**, 31 (1985).

[11] C. Meneveau, K. R. Sreenivasan, P. Kailasnath and M. S. Fan, Phys. Rev. A **41**, 894 (1990).

[12] J. L. Synge and C. C. Lin, Trans. Roy. Soc. Can. **37**, 45 (1943).

[13] A. J. Chorin, Vorticity and Turbulence, Springer-Verlag, 1991.

[14] P. G. Saffman and D. I. Pullin, Phys. Fluids, **8**, 3072 (1996); D. I. Pullin and P. G. Saffman, Annu. Rev. Fluid Mech. **30**, 31 (1998).

[15] V. S. Lvov, E. Podivilov, and I. Procaccia, Phys. Rev. Lett. **79**, 2050 (1997).

[16] A. Vincent and M. Meneguzzi, J. Fluid Mech. **225**, 1 (1991).

[17] J. M. Burgers, Adv. Appl. Mech **1**, 45 (1948).

[18] H. K. Moffatt, S. Kida and K. Ohkitani, J. Fluid Mech. **259**, 241 (1994).

[19] J. Jiménez, A. A. Saffman, P. G. Saffman and R. S. Rogallo, J. Fluid Mech. **255**, 63 (1993).

[20] N. Hatakeyama and T. Kambe, Phys. Rev. Lett., **79**, 1257 (1997).

[21] F. Belin, J. Maurer, P. Tabeling and H. Willaime, J. Phys. II France **6**, 573 (1996).

[22] A. N. Kolmogorov, C. R. Acad. Sci. URSS **30**, 301 (1941).

[23] K. R. Sreenivasan and R. A. Antonia, Annu. Rev. Fluid Mech., **29**, 435 (1997).

[24] A. M. Obukhov, J. Fluid Mech. **13**, 77 (1962); A. N. Kolmogorov, J. Fluid Mech. **13**, 82 (1962).

[25] B. Dubrulle, J. Phys. II France **6** 1825 (1996); G. He and B. Dubrulle, J. Phys. II France **7** 793 (1997).